J Pharmacol Sci **101**, 214 – 222 (2006)

Journal of Pharmacological Sciences

Full Paper

Acetylcholine Inhibits the Hypoxia-Induced Reduction of Connexin43 Protein in Rat Cardiomyocytes

Yanan Zhang[1], Yoshihiko Kakinuma[2,*], Motonori Ando[2], Rajesh G Katare[2], Fumiyasu Yamasaki[1], Tetsuro Sugiura[1], and Takayuki Sato[2]

Departments of [1]Clinical Laboratory and [2]Cardiovascular Control, Kochi Medical School, Nankoku, Kochi 783-8505, Japan

Received December 14, 2005; Accepted May 8, 2006

Abstract. In a recent study, we demonstrated that vagal stimulation increases the survival of rats with myocardial infarction by inhibiting lethal arrhythmia through regulation of connexin43 (Cx43). However, the precise mechanisms for this effect remain to be elucidated. To investigate these mechanisms and the signal transduction for gap junction regulation, we investigated the effect of acetylcholine (ACh), a parasympathetic nerve system neurotransmitter, on the gap junction component Cx43 using H9c2 cells. When cells were subjected to hypoxia, the total Cx43 protein level was decreased. In contrast, pretreatment with ACh inhibited this effect. To investigate the signal transduction, cells were pretreated with L-NAME, a nitric oxide synthase inhibitor, followed by ACh and hypoxia. L-NAME was found to suppress the ACh effect. However, a NO donor, SNAP, partially inhibited the hypoxia-induced reduction in Cx43. To delineate the mechanisms of the decrease in Cx43 under hypoxia, cells were pretreated with MG132, a proteasome inhibitor. Proteasome inhibition produced a striking recovery of the decrease in the total Cx43 protein level under hypoxia. However, cotreatment with MG132 and ACh did not produce any further increase in the total Cx43 protein level. Functional studies using ACh or okadaic acid, a phosphatase inhibitor, revealed that both reagents inhibited the decrease in the dye transfer induced by hypoxia. These results suggest that ACh is responsible for restoring the decrease in the Cx43 protein level, resulting in functional activation of gap junctions.

Keywords: acetylcholine, connexin43, cardiomyocyte, hypoxia, proteasome inhibitor

Introduction

The prognosis of patients with chronic heart failure remains poor, despite the introduction of new pharmacological approaches and defibrillation devices, mainly due to lethal arrhythmia (1). Therefore, another therapeutic approach would be indispensable. In heart failure, the sympathetic nerve system is relatively activated compared with the parasympathetic nerve system (2), and this sympathetic nerve system-predominant condition is known to be involved in arrhythmogenicity. Recently, vagal nerve stimulation was reported to remarkably improve the survival rate of rats with heart failure due to myocardial infarction (3), suggesting that reactivation of the parasympathetic nerve system, which is suppressed in heart failure, plays a crucial role in attenuating the progression of heart failure. Moreover, our recent study revealed that acetylcholine (ACh), a parasympathetic nerve system neurotransmitter, plays an important role in regulating the protein level of the gap junction component connexin43 (Cx43) in the infarcted heart and cardiomyocytes under hypoxia (4). However, the precise mechanisms by which ACh regulates Cx43 remain to be elucidated. To investigate these mechanisms, we focused on Cx43 in H9c2 cells.

Gap junctions are intercellular junctions, and several connexin family members, including Cx43, participate in their formation. Among the connexin family members, Cx43 is the principal electrical coupling

*Corresponding author. kakinuma@med.kochi-u.ac.jp
Published online in J-STAGE: July 7, 2006
doi: 10.1254/jphs.FP0051023

protein in ventricles, while Cx40 plays the same role in atria. The functions of Cx43 are regulated by phosphorylation as well as the protein level. Cx43 phosphorylation can modulate the channel properties and turnover dynamics. SDS-PAGE of Cx43 generally reveals a faster non-phosphorylated isoform (NP-Cx43) and slower phosphorylated isoforms (P-Cx43). Cx43 is synthesized in the rough endoplasmic reticulum, transported to the Golgi apparatus, and ultimately trafficked to the plasma membrane (5, 6). Recent evidence has suggested that Cx43 is involved in modifying arrhythmogenic conditions (7, 8) since Cx43 knockout mice were subject to sudden death caused by lethal arrhythmia, including ventricular tachycardia, or fibrillation (9, 10). Although many other factors, including sodium, potassium, and calcium channels, appear to be involved in arrhythmogenicity, it is speculated that functional deletion of Cx43 is also responsible for arrhythmia. To date, it has remained unclear whether and how ACh modulates Cx43. Therefore, we focused on the effect of ACh on Cx43.

Materials and Methods

Cell culture and pharmacological agents

H9c2 cells, which are spontaneously immortalized ventricular myoblasts from rat embryos, were used due to their conserved electrical and signal transduction characteristics (11). The cells were cultured in DMEM supplemented with 10% FBS and antibiotics. H9c2 cells were pretreated with 1 mM ACh for 8 h, followed by 1 h of hypoxia (1% of oxygen concentration). We chose N^{ω}-nitro-L-arginine methyl ester (L-NAME) (Sigma Chemical Co., St Louis, MO, USA), a specific nitric oxide (NO) synthase inhibitor, to determine whether NO mediates the signal transduction for Cx43 expression. L-NAME (1 mM) was administered for 1 h together with ACh, followed by hypoxia for 1 h. H9c2 cells were also treated with 1 mM *S*-nitroso-*N*-acetyl-l,l-penicillamine (SNAP) (Sigma Chemical Co.) before hypoxia. We used 10 μM Cbz-leu-leu-leucinal (MG132) (Sigma Chemical Co.) or 1 μM okadaic acid to investigate whether hypoxia enhanced Cx43 degradation or phosphorylation was important for regulating the functional activity of Cx43.

Western blot analysis

Cells were harvested from the dishes and prepared for immunoblotting as described previously (8). After washing in PBS, cells were lysed with SDS sample buffer and boiled for 10 min. After electrophoresis in a 10% SDS-polyacrylamide gel, proteins were transferred to a polyvinylidene difluoride membrane. The membrane was soaked in 4% skim milk in TBST solution overnight, then incubated with an anti-Cx43 polyclonal antibody (ZYMED Laboratories, Inc., South San Francisco, CA, USA) for 1 h, thoroughly washed, and then incubated with an anti-rabbit IgG secondary antibody (BD Transduction Laboratories, San Diego, CA, USA) for 40 min. Finally, the membrane was washed and subjected to chemiluminescent detection using the ECL Plus Western Blotting Detection Reagents (Amersham Biosciences, Piscataway, NJ, USA). We performed repeatedly 3-5 times each experiment using duplicate samples. The Western blotting data were analyzed using Kodak 1D Image Analysis Software (Eastman Kodak Co., Rochester, NY, USA).

Immunohistochemistry

H9c2 cells were fixed with 4% paraformaldehyde for 10 min and permeabilized with 1% Triton X-100 for another 10 min. To block nonspecific antibody binding, cells were incubated with 5% skim milk and successively incubated with an anti-Cx43 polyclonal antibody (ZYMED Laboratories, Inc.), in 1% skim milk at 4°C overnight and then with a Cy3-labeled secondary antibody (Jackson ImmunoReserch Laboratories, West Grove, PA, USA) at 4°C overnight. Actin staining was performed using FITC-conjugated phalloidin and then examined with a laser scanning confocal microscope.

Functional analysis of gap junction using a scrape and scratch method

A scrape-loading method can be used to introduce macromolecules into cultured cells by inducing a transient tear in the plasma membrane without affecting cell viability, thereby allowing sensitive determination of cell-cell communication. Following the treatment with ACh or okadaic acid, cells cultured on a coverslip were rinsed with PBS, and then 1% Lucifer Yellow was applied to the center of the coverslip. A 27 gauge needle was used to create two longitudinal scratches through the cell monolayer. The cells were incubated in the dye mix for exactly 1 min, quickly rinsed three times with PBS, and finally examined by fluorescence microscopy. Lucifer Yellow does not diffuse through intact plasma membranes, but its low molecular weight permits its transmission from one cell to another, presumably across patent gap junctions (12 – 16). The area of the dye transferred from the scratched margin in hypoxia or hypoxia with ACh treatment was semi-quantified using the NIH image system and compared with that in normoxia.

Statistical analyses

Data are presented as the mean ± S.E.M. Differences

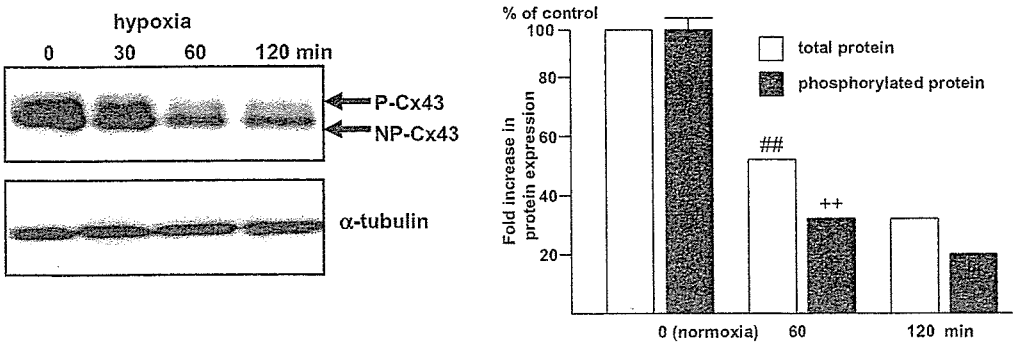

Fig. 1. Cx43 phosphorylation is decreased by hypoxia. Cells are subjected to 30 – 120 min of hypoxia and then analyzed by Western blot analysis. Cx43 phosphorylation (P-Cx43) is reduced to 32 ± 4% of the level under normoxia ($^{++}P<0.01$ *vs* 0 min, $^{\#\#}P<0.01$ *vs* 0 min) by 1% hypoxia, and the effect is remarkable after 60 min of hypoxia. NP-Cx43: non-phosphorylated form of Cx43. Open bars: total Cx43 protein level, closed bars: P-Cx43 level. Representative data from 5 independently performed experiments are shown (n = 5).

were assessed by ANOVA followed by Fisher's PLSD for multiple comparisons. The results were considered statistically significant at the level of $P<0.05$.

Results

Hypoxia decreases the Cx43 protein level in H9c2 cells

Several different forms of Cx43 were observed in the case of H9c2 cell (Fig. 1). The upper bands represented the phosphorylated forms, while the lower band corresponded to the non-phosphorylated form. We examined the acute effect of hypoxia on the total Cx43 protein level in H9c2 cells (n = 5). The total protein level of Cx43, including NP-Cx43 and P-Cx43, gradually decreased during hypoxia (Fig. 1), and 60 min of hypoxia induced a remarkable decrease in the total Cx43 protein level ($^{\#\#}P<0.01$ *vs* 0 min of hypoxia) and reduced its phosphorylation to 32 ± 4% of the normoxic level ($^{++}P<0.01$ *vs* 0 min of hypoxia). These results suggest that the total Cx43 protein level is rapidly decreased under hypoxia.

ACh increases the Cx43 protein level in H9c2 cells under normoxia or hypoxia

To determine whether ACh could modulate the Cx43 protein level after acute treatment, we initially treated H9c2 cells with 1 mM ACh under normoxia (n = 3). When the cells were stimulated with 1 mM ACh under normoxia, the Cx43 protein level was transiently increased ($^{++}P<0.01$ *vs* 0 min), followed by a rapid decrease, and then another peak was observed at 8 h (Fig. 2A). Next, to examine the effect of ACh on the hypoxia-induced decrease in Cx43, we pretreated H9c2 cells with 1 mM of ACh for 7 h, followed by 1 h of hypoxia (n = 6). Compared to the Cx43 level under hypoxia alone (hypoxia), the Cx43 protein level in ACh-pretreated H9c2 cells was not decreased under hypoxia (ACh + hypoxia), but instead was rather sustained ($^{\#\#}P<0.01$ *vs* hypoxia; ns, not significant *vs* normoxia; n = 6) (Fig. 2B). This ACh-mediated inhibition of the decrease in Cx43 under hypoxia was also observed by immunocytochemistry since hypoxia decreased the Cx43 immunoreactivity, and ACh inhibited the reduction (Fig. 2C).

Inhibition of the decrease in the Cx43 protein level during hypoxia by ACh occurs via NO

To further characterize the signal transduction for ACh-mediated inhibition of the reduction in the Cx43 protein level under hypoxia, we investigated the effects of chemicals on the Cx43 protein level (n = 5) (Fig. 3). Pretreatment with L-NAME (1 mM) for 1 h inhibited the ACh-induced recovery of the Cx43 protein level during hypoxia, suggesting that NO participates in regulating the Cx43 protein level ($^{\#}P<0.05$ *vs* ACh, n = 5). To further investigate whether the protein level was affected by NO, the cells were treated with 1 mM SNAP, a NO donor, instead of ACh. SNAP partially inhibited the reduction in the Cx43 protein level compared with L-NAME treatment, further suggesting that NO plays a partial role in modulating the protein level ($^{+}P<0.05$ *vs* L-NAME, n = 5).

Cx43 is degraded under hypoxia

To further investigate the mechanisms of the decrease in Cx43 under hypoxia, H9c2 cells were pretreated with the proteasome inhibitor MG132 (n = 5) for 10 and 60 min during hypoxia (Fig. 4A). The proteasome inhibition produced a striking recovery of the decreased total Cx43 protein level. MG132 inhibited the reduction

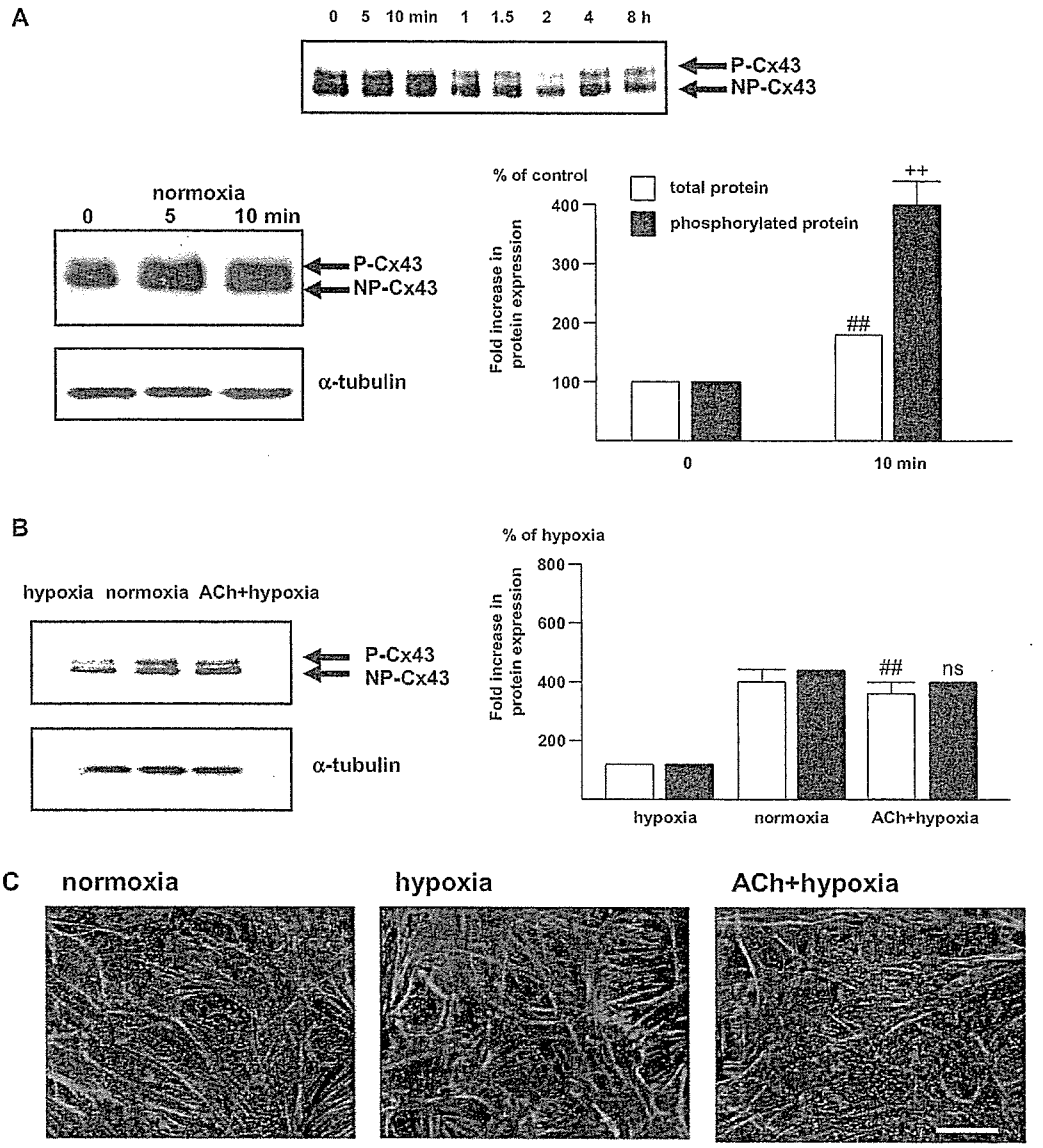

Fig. 2. ACh regulates Cx43 phosphorylation under normoxia and hypoxia. A: 1 mM ACh increases Cx43 phosphorylation (P-Cx43) in the acute phase under normoxia, reaching a peak of 409 ± 28% at 10 min ($^{++}P<0.01$ *vs* 0 min, $^{\#\#}P<0.01$ *vs* 0 min, n = 3). The entire time course shows another peak of the Cx43 protein level following the acute phase at 8 h. B: ACh suppresses the reduction in the Cx43 protein level induced by 1 h of hypoxia. ACh (1 mM) pretreated H9c2 cells show a sustained level of Cx43 phosphorylation, comparable to that under normoxia (normoxia), even under hypoxia (ACh + hypoxia) ($^{\#\#}P<0.01$ *vs* hypoxia; ns, not significant *vs* normoxia; n = 6). C: ACh inhibits the reduction in Cx43 immunoreactivity under hypoxia (red dots). Representative staining is shown. Cx43 is indicated by red dots. Bar: 50 μm.

in the Cx43 protein level by hypoxia for up to 60 min, suggesting that the reduction is due to activation of Cx43 protein degradation ($^{\#}P<0.05$ *vs* normoxia, n = 5). Furthermore, the effect of MG132 on inhibiting Cx43 degradation was not modified by ACh addition, and as a consequence, the effect of MG132 on inhibiting the hypoxia-induced decrease in Cx43 was comparable to that of cotreatment with MG132 and ACh (not significant *vs* ACh + MG132, n = 5) (Fig. 4B). These results suggest that ACh modulates the degradation process of Cx43.

ACh activates the function of gap junctions through an increase in the Cx43 protein level

To investigate whether ACh inhibition of the Cx43 protein level during hypoxia leads to functional recovery of gap junctions, we applied the scrape/scratch technique (n = 5). In a control experiment, scrape-loaded

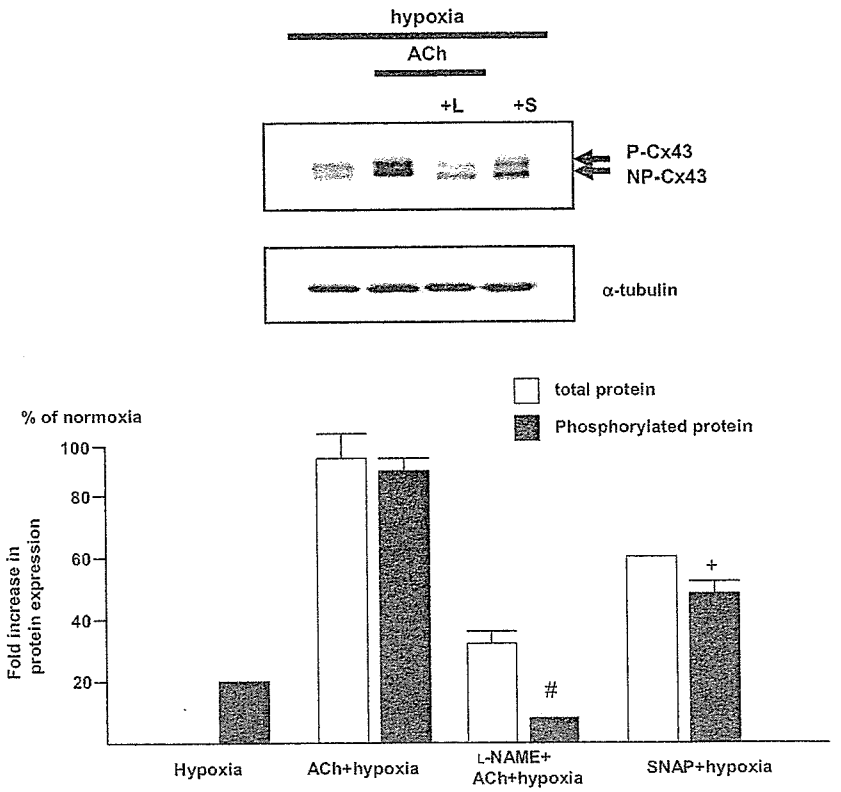

Fig. 3. NO is involved in the ACh signaling pathway that leads to the increase in Cx43 phosphorylation ($^{\#}P<0.05$ *vs* ACh + hypoxia; $^{+}P<0.05$ *vs* L-NAME + ACh + hypoxia). ACh: 1 mM ACh, L: 1 mM L-NAME, S: 1 mM SNAP. Representative data from 5 independently performed experiments are shown (n = 5).

cells in the presence of Lucifer Yellow showed positive transfer of Lucifer Yellow between cells. In contrast, cells treated with hypoxia appeared to lose their ability to communicate with each other and the dye transfer was blocked to 6 ± 2% of the intensity under normoxia. In contrast, ACh suppressed the hypoxia-induced blockage of dye transfer ($^{\#\#}P<0.01$ *vs* hypoxia, not significant *vs* normoxia, n = 5). The area of Lucifer Yellow fluorescence was increased in ACh-treated cells along the scraped margin during hypoxia (62 ± 10% of the area under normoxia) (Fig. 5). These results suggest that hypoxia affects intercellular communication and that ACh functionally activates cell-cell communication, even under hypoxia, through increases in the Cx43 protein level. Furthermore, pretreatment with 1 μM okadaic acid, a phosphatase inhibitor, for 10 min recovered the reduction in the Cx43 protein level and the extent of dye transfer during hypoxia (Fig. 6). Taken together with the results obtained with the proteasome and phosphatase inhibitors, it is suggested that both the protein and phosphorylation levels of Cx43 are involved in the function of Cx43.

Discussion

In the current study, we have shown that the Cx43 protein level is regulated by ACh in the presence or absence of hypoxia. Even in normoxia, ACh regulated the Cx43 protein level and inhibited the reduction in the Cx43 protein level induced under hypoxia. Such modification of the Cx43 protein level by ACh partially occurred via NO, since the protein level sustained by ACh during hypoxia was affected by L-NAME, whereas SNAP showed similar effects to ACh. Furthermore, the results indicated that the hypoxia-induced decrease in the total Cx43 protein level is due to proteasome degradation. Taken together, these results further suggest that ACh is involved in inhibiting Cx43 degradation under hypoxia.

Our previous study revealed that vagal stimulation inhibited the reduction in the Cx43 protein level during acute myocardial ischemia and instead sustained a similar level to that in the normal heart (4). As a result, vagal stimulation was further shown to decrease the frequency of ventricular arrhythmia. Moreover, ACh sustained the dye transfer level, which was attenuated

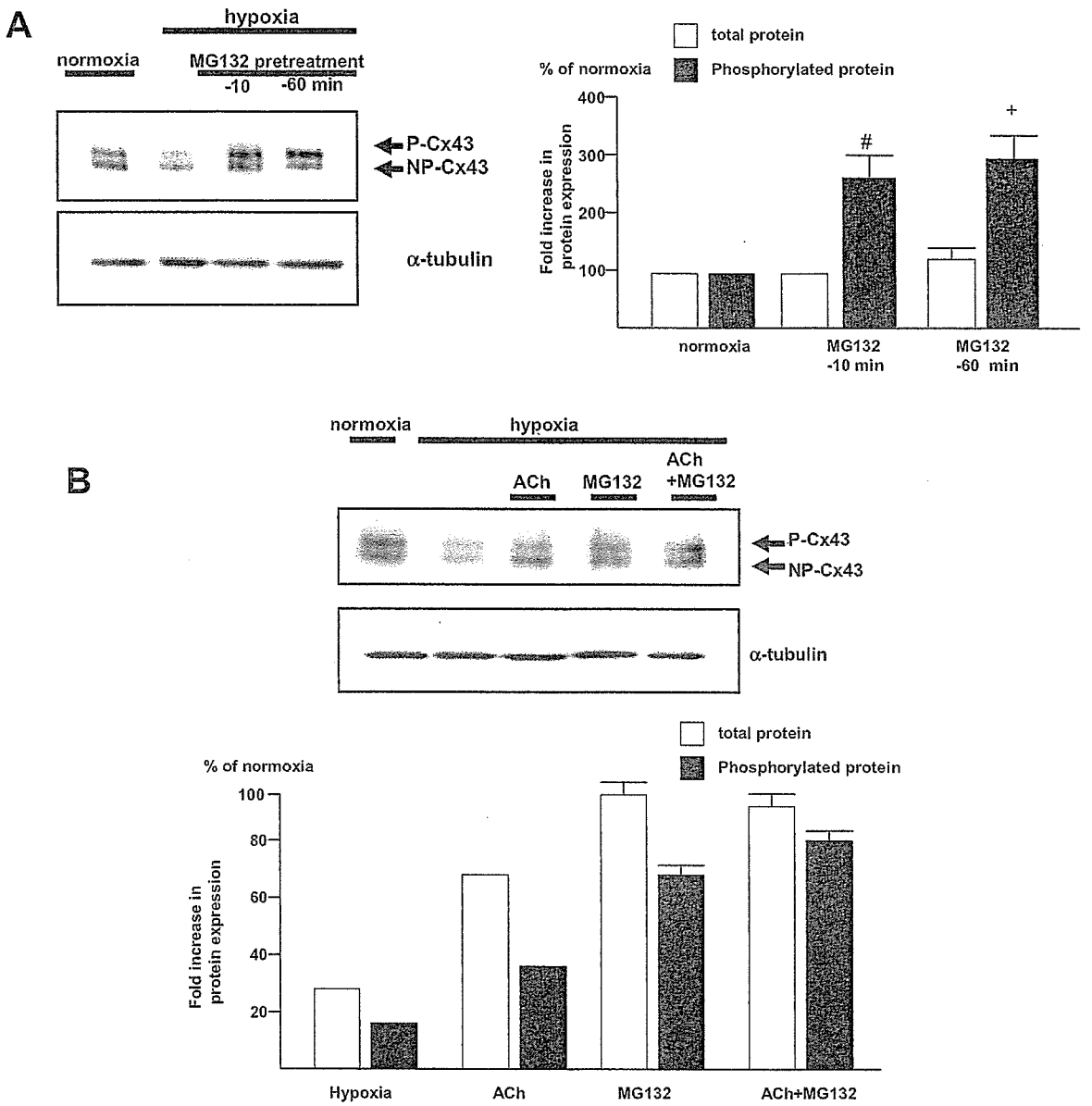

Fig. 4. MG132, a proteasome inhibitor, increases the Cx43 protein level during hypoxia, and cotreatment with ACh does not change this effect. A: Pretreatment with MG132 inhibits the reduction in Cx43 phosphorylation induced by hypoxia ($^{\#}P<0.05$ *vs* normoxia; $^{+}P<0.05$ *vs* normoxia, n = 5). Normoxia: no MG132 or hypoxia. The cells were pretreated with 10 μmol/L MG132 before and at 10 and 60 min of hypoxia. B: The effect of MG132 on inhibiting the reduction in Cx43 phosphorylation is not accentuated by cotreatment with 1 mM ACh since the level of Cx43 phosphorylation with ACh + MG132 is comparable to that with MG132 alone (not significant *vs* MG132, n = 5). Representative data from 5 independently performed experiments are shown (n = 5).

under hypoxia, to the same level observed under normoxia. On the basis of the finding that the survival of Cx43 knockout mice was extremely poor due to ventricular arrhythmia (9, 10), it is suggested that ACh regulates Cx43, which may inhibit arrhythmia.

Our immunohistochemical study supported the result that ACh greatly suppressed the reduction in the Cx43 level under hypoxia. L-NAME inhibited the effect of ACh on Cx43, whereas SNAP mimicked the ACh effect, suggesting that NO is involved in the signaling pathway. ACh is able to induce NO production (17) and has a cardioprotective effect both in vivo and in vitro (18, 19). In fact, H9c2 cells were reported to generate NO from mitochondria in response to ACh (20). Taken together,

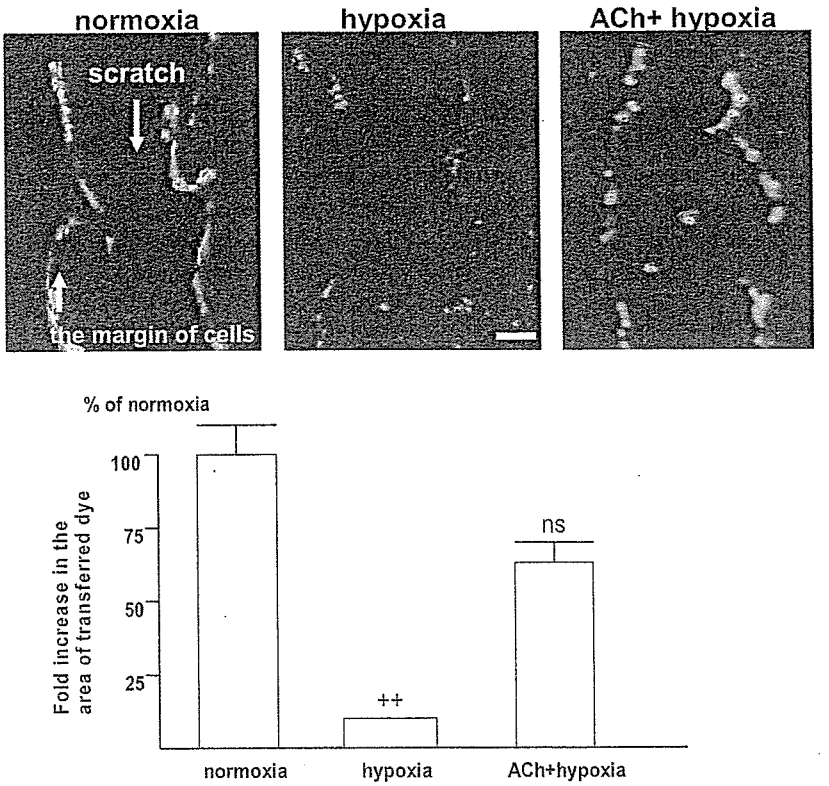

Fig. 5. Fluorescence photomicrographs of scrape/scratch experiments using Lucifer Yellow. Intercellular communication is blocked in H9c2 cells treated with 60 min of hypoxia (hypoxia) ($^{++}P<0.01$ *vs* hypoxia, n = 5). ACh (1 mM) reverses the blockage of intercellular communication induced by hypoxia (ACh + hypoxia) to a comparable level to the control (ns, not significant *vs* normoxia; n = 5) Bar: 150 μm.

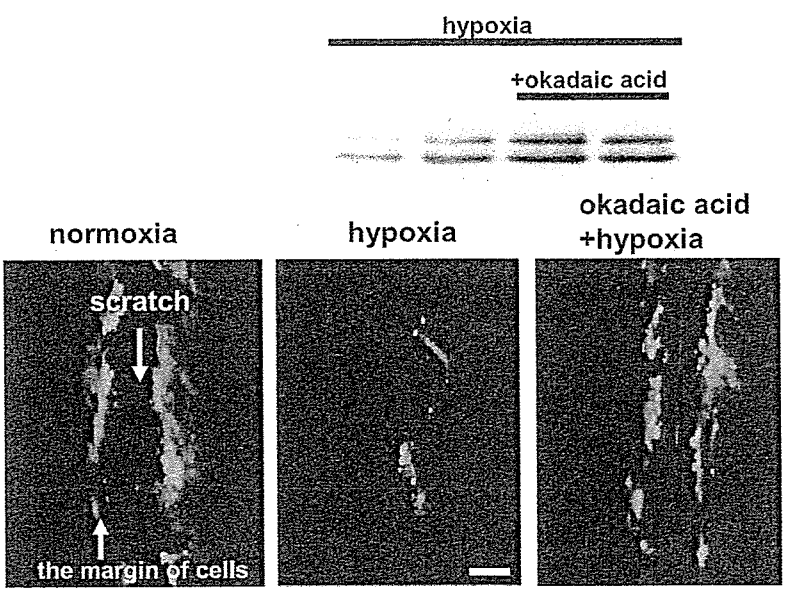

Fig. 6. Phosphatase inhibition recovers cell-cell communication during hypoxia. Pretreatment with okadaic acid (1 μm) for 10 min before hypoxia inhibits the reduction in the Cx43 protein level during hypoxia. Furthermore, it reverses the dye transfer blockage under hypoxia, similar to ACh. Representative data from 3 independently performed experiments are shown (n = 3). Bar: 150 μm.

it is suggested that ACh regulates the Cx43 protein level in cardiomyocytes partly through NO.

To explore whether the Cx43 level during hypoxia was regulated by proteasome degradation, we treated cells with the proteasome inhibitor MG132. Recently, several types of low-molecular-weight proteasome inhibitors have been developed that can readily enter cells and selectively inhibit the protein-degradation pathway. Although their toxicities may sometimes be troublesome experimentally, cell viability and growth are not generally affected by short treatments with these molecules (21 – 23). Surprisingly, MG132 increased the Cx43 protein level, which was reduced under hypoxia, to a comparable level to that after ACh treatment. However, the effect of MG132 on the recovery of Cx43 was not affected by cotreatment with ACh. These results suggest that the proteasome pathway plays a role in Cx43 degradation and that ACh modulates the degradation of Cx43 during hypoxia.

The results of the present study have demonstrated that the increased Cx43 protein level contributes to the functional improvement of gap junctions under hypoxia using the scrape/scratch method. The ACh-induced increase in the Cx43 protein level was functionally involved in the cell-cell communication since ACh recovered Lucifer Yellow transport from the margin of the scratched regions, even under in hypoxia.

As well as the total protein level, the Cx43 phosphorylation level was shown to be involved in its function. Specifically, okadaic acid, a phosphatase inhibitor, recovered the Cx43 protein level and the extent of dye transfer under hypoxia, suggesting that dephosphorylation was partially involved in the hypoxia-induced degradation, eventually leading to a decrease in the total Cx43 protein level. To date, several phosphorylation sites of Cx43 have been reported to have positive or negative effects on gap junctions, suggesting that their function depends on these phosphorylation sites (24). Although we did not investigate the specific phosphorylation site regulated by ACh in the present study, our results suggest that ACh modulates the function of gap junctions through both the protein and phosphorylation levels of Cx43.

Although the scrape/scratch method has some limitations for evaluating cell-cell communication, the result obtained were compatible with those in our previous dye injection study under chemical hypoxia, that is, ACh-treated cardiomyocytes efficiently transferred the dye to surrounding cells, even under hypoxia (4). Therefore, these results suggest that inhibition of the decrease in the Cx43 protein level by ACh under hypoxia is responsible for the enhanced cell-cell communication.

H9c2 cells have been shown to retain several characteristics of the electrical and hormonal signaling pathways found in adult cardiomyocytes and are therefore a useful model for cardiomyocytes from the aspect of signal transduction. The cells show similar morphological characteristics to immature embryonic cardiomyocytes (20).

In conclusion, the results of the present study suggest that ACh activates cell-cell communication by sustaining the Cx43 protein level during hypoxia through modification of the Cx43 degradation pathway.

Acknowledgment

This study was supported by a Health and Labor Sciences Research Grant (H15-PHYSI-001) for Advanced Medical Technology from Ministry of Health, Labor, and Welfare of Japan.

References

1 Janse MJ. Electrophysiological changes in heart failure and their relationship to arrhythmogenesis. Cardiovasc Res. 2004;61:208–217.
2 Prado MAM, Reis RAM, Prado VF, de Mello MC, Gomez MV, de Mello PG. Regulation of acetylcholine synthesis and storage. Neurochem Int. 2002;41:291–299.
3 Li M, Zheng C, Sato T, Kawada T, Sugimachi M, Sunagawa K. Vagal nerve stimulation markedly improves long-term survival after chronic heart failure in rats. Circulation. 2004;109:120–124.
4 Ando M, Katare GR, Kakinuma Y, Zhang D, Yamasaki F, Muramoto K, et al. Efferent vagal nerve stimulation protects heart against ischemia-induced arrhythmias by preserving connexin43 protein. Circulation. 2005;12:164–170.
5 Musil LS, Goodenough DA. Biochemical analysis of connexin43 intracellular transport, phosphorylation, and assembly into gap junctional plaques. J Cell Biol. 1991;115:1357–1374.
6 Lamp PD, Lau AF. Regulation of gap junctions by phosphorylation of connexins. Arch Biochem Biophys. 2000;384:205–215.
7 Moon C-H, Jung Y-S, Kim MH, Park RM, Lee SH, Baik EJ. Protein kinase C inhibitors attenuate protective effect of high glucose against hypoxic injury in H9c2 cardiac cells. Jpn J Physiol. 2000;50:645–649.
8 Jain SK, Schuessler RB, Saffitz JE. Mechanisms of delayed electrical uncoupling induced by ischemic preconditioning. Circ Res. 2003;92:1138–1144.
9 van Rijen HV, Eckardt D, Degen J, Theis M, Ott T, Willecke K, et al. Slow conduction and enhanced anisotropy increase the propensity for ventricular tachyarrhythmias in adult mice with induced deletion of connexin43. Circulation. 2004;109:1048–1055.
10 Gutstein DE, Morley GE, Vaidya D, Liu F, Chen FL, Stuhlmann H, et al. Conduction slowing and sudden arrhythmic death in mice with cardiac-restricted inactivation of connexin43. Circ Res. 2001;88:333–339.

11 Hescheler J, Meyer R, Plant S, Krautwurst D, Rosenthal W, Rosenthal W, et al. Morphological, biochemical, and electrophysiological characterization of a clonal cell (H9c2) line from rat heart. Circ Res. 1991;69:1476–1486.
12 Le A-CN, Musil LS. Normal differentiation of cultured lens cells after inhibition of gap junction-mediated intercellular communication. Dev Biol. 1998;204:80–96.
13 Musil LS, Le A-CN, Vanslyke JK, Roberts LM. Regulation of connexin degradation as a mechanism to increase gap junction assembly and function. J Biol Chem. 2000;275:25207–25215.
14 McNeil PL, Murphy RF, Lanni F, Taylor DL. A method for incorporating macromolecules into adherent cells. J Cell Biol. 1984;98:1556–1564.
15 El-Fouly MH, Trosko JE, Chang C-C. Scrape-loading and dye transfer. A rapid and simple technique to study gap junctional intercellular communication. Exp Cell Res. 1987;168:422–430.
16 Stewart WW. Functional connections between cells as revealed by dye-coupling with a highly fluorescent naphthalimide tracer. Cell. 1978;14:741–759.
17 Liu H, Mcpherson BC, Zhu X, Da Costa MA, Jeevanandam V, Yao Z. Role of nitric oxide and protein kinase C in ACh-induced cardioprotection. Am J Physiol Heart Circ Physiol. 2001;281: H191–H197.
18 Rakhit R, Edwards RJ, Mockridge JW, Baydoun AR, Wyatt AW, Mann GE, et al. Nitric oxide, nitrates and ischaemic preconditioning. Am J Physiol Heart Circ Physiol. 2000;278: H1211–H1217.
19 Monastyrskaya E, Folarin N, Malyshev I, Green C, Andreeva L. Application of the nitric oxide donor SNAP to cardiomyocytes in culture provides protection against oxidative stress. Nitric Oxide. 2002;7:127–131.
20 Zanella B, Calonghi N, Pagnotta E, Masotti L, Guarnieri C. Mitochondrial nitric oxide localization in H9c2 cells revealed by confocal microscopy. Biochem Biophys Res Commun. 2002;290:1010–1014.
21 Lee DH, Goldberg AL. Proteasome inhibitors: valuable new tools for cell biologists. Trends Cell Biol. 1998;8:397–403.
22 Laing JG, Beyer EC. The gap junction protein connexin43 is degraded via the ubiquitin proteasome pathway. J Biol Chem. 1995;270:26399–26403.
23 Lampe PD, Tenbroek EM, Brut JM, Kurata WE, Johnson RG, Lau AF. Phosphorylation of connexin43 on serine368 by protein kinase C regulates gap junctional communication. J Cell Biol. 2000;149:1503–1512.
24 Lampe PD, Lau AF. The effects of connexin phosphorylation on gap junctional communication. Int J Biochem Cell Biol. 2004;36:1171–1186.

バイオニック治療戦略

高知大学循環制御学 佐藤隆幸
九州大学大学院医学研究院循環器内科学 砂川賢二

はじめに

循環器疾患では，心不全や圧反射失調のように制御機構の機能破綻が病態の悪化や予後を規定する因子になることがある．そこで，積極的に循環制御機構の機能再建や最適化を図るための新しい治療戦略として，神経インターフェイス技法を用いたバイオニック療法が提唱されている[1]．

本稿では迷走神経の電気刺激による心不全治療[2]に関する実験的研究，および脊髄交感神経刺激による術中自動血圧制御に関する臨床研究[3]について紹介する．

迷走神経刺激による慢性心不全治療

最新の病態に関する研究により，慢性心不全の重要な予後規定因子として，循環調節機構の破綻があげられている．当初は，心機能低下の代償機転として適応的にはたらいていた交感神経系の活性化と副交感神経系の活動低下やレニン・アンジオテンシン系の活性化が，次第に心臓リモデリングを進展・悪化させ，一種の悪循環を形成し，最終的には調節破綻に陥ると考えられるようになってきた．さらに，大規模臨床試験により，呼吸性心拍変動の低下や心拍数増加が予後不良因子として認識されるようになった．これらはいずれも心臓迷走神経活動の低下を反映したものである[4~8]．そこで，「迷走神経を電気刺激する神経インターフェイス療法」が生命予後を改善するか否かを心不全モデル動物を用いて実験的に検証した．

左冠動脈起始部の結紮により，左室の40～50％が梗塞に陥った慢性心不全ラットの右迷走神経に刺激電極を固定し，植え込み型電気刺激装置と接続した．刺激強度は心拍数が10～20％低下する程度にした．迷走神経刺激療法は6週間でうち切り，血行動態・心臓リモデリングに与える影響と140日間の長期生存率を観察した．

1. 心機能およびリモデリングに与える影響

図1は治療終了時の血行動態の比較を示している．血圧は，梗塞後心不全群は健常群に比べ有意に低かった．梗塞後心不全群は，健常群に比べ左室拡張末期圧の有意な上昇と左室圧一次微分最大値の有意な低下を示したが，迷走神経刺激療法により，左室拡張末期圧の有意な減少と左室圧一次微分最大値の有意な上昇が認められた．両心室重量が，梗塞後心不全群では有意な増加を示したが，迷走神経刺激療法により有意に減少した．以上の結果は，6週間の迷走神経刺激療法によってポンプ機能が改善し心室リモデリングが予防されたことを示唆する．

[Key words] 循環調節，迷走神経，交感神経，神経インターフェイス

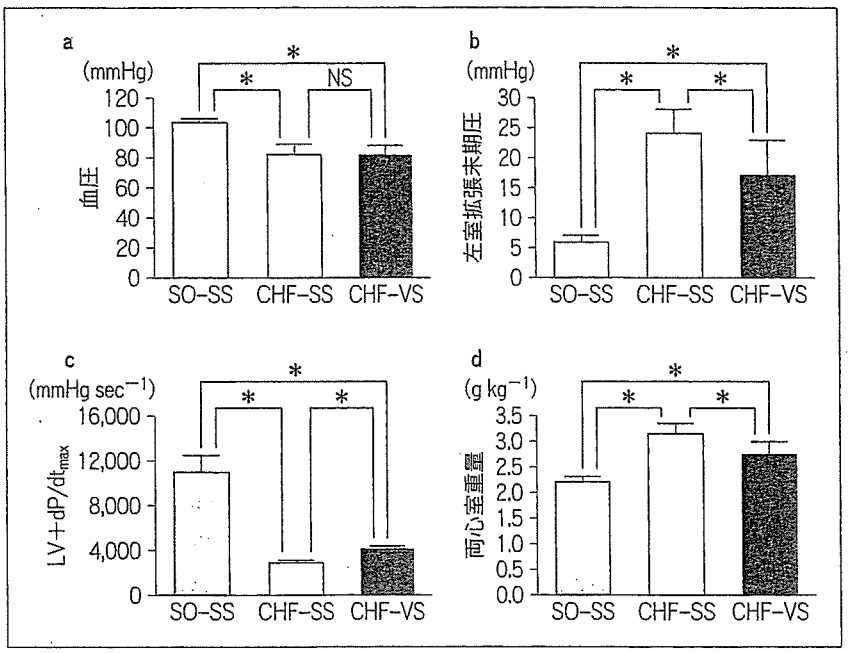

図1　迷走神経刺激の血行動態および両心室重量に与える影響

健常群（SO-SS, $n=9$），梗塞後心不全における非刺激群（CHF-SS, $n=13$）および梗塞後心不全における刺激群（CHF-VS, $n=11$）．数値は平均±標準偏差で示している．*$p<0.05$.

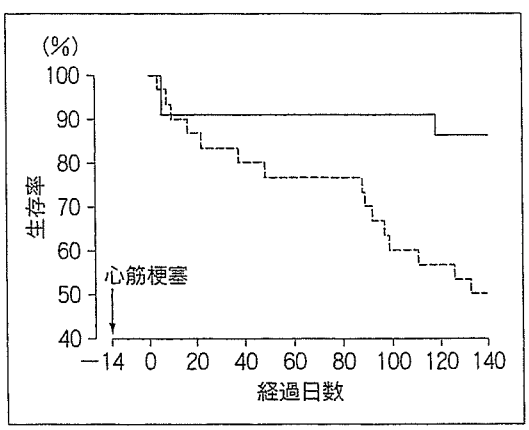

図2　迷走神経刺激の慢性心不全ラットの生存率に与える影響

実線は刺激群（$n=22$），破線は非刺激群（$n=30$）を示す．迷走神経刺激により生存率は有意に改善した（$p=0.008$）．

期間における生存率曲線を図2に示す．刺激群22例のうち死亡は3例，非刺激群30例のうち死亡は15例であった（$p=0.008$）．このように，迷走神経刺激療法は相対的死亡リスクを73%も減少させた．この効果は，アンジオテンシン変換酵素阻害薬によるものよりもさらに良好な成績であった[9]．

迷走神経刺激療法は，両心室重量，血漿ノルエピネフリンおよび脳性ナトリウム利尿ペプチドを有意に減少させた．なお，これらの指標はいずれも臨床試験で明らかにされている予後規定因子で，高値ほど予後不良とされているものである．

以上より，迷走神経刺激療法が心機能の改善とリモデリングを予防し，さらに，長期予後を著明に改善することが明らかになった[2]．

2.　長期生存率および液性因子に与える影響

迷走神経刺激療法の生存率に与える影響をKaplan-Meier法により解析した．140日の観察

3.　迷走神経刺激による抗リモデリング機序

迷走神経刺激により，不全心で生ずるリモデリングが予防される機序として，徐脈によりエネル

ギー効率の改善[10]，冠循環における血管内皮機能の改善[11]などが考えられるが，不明なところも多い．最近，筆者らは，迷走神経の末端から放出されるアセチルコリンが心筋細胞に与える影響について調べたところ，アセチルコリンがムスカリン受容体を介して，低酸素誘導因子 HIF-1α の発現を促進し，不全心でみられるアポトーシスを防止する可能性があることを報告した[12]．また，末期心不全における致死性不整脈との関連が示唆されているギャップ結合の機能低下を迷走神経刺激が防止する可能性があることを示した[13]．おもしろいことに，これらの迷走神経あるいはアセチルコリンの心筋細胞に与える効果は，徐脈効果とは独立した機序である可能性がある．

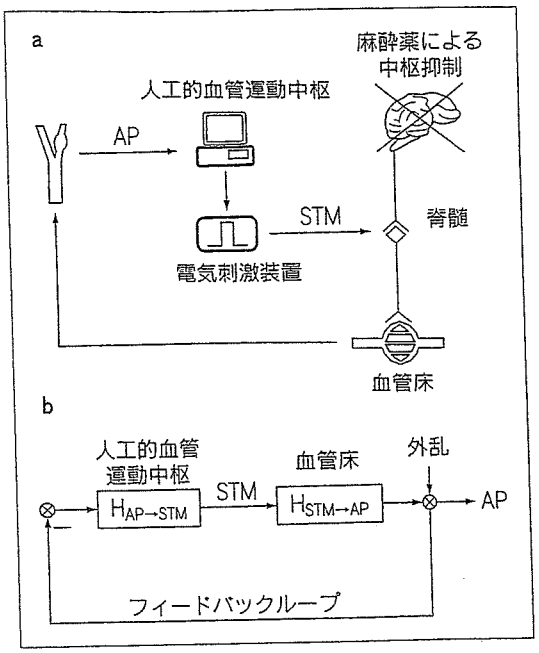

図3　バイオニック圧反射装置
バイオニック圧反射装置の概要（a）とブロック線図（b）．AP と STM はそれぞれ血圧と電気刺激を示す．

脊髄交感神経刺激による術中血圧の自動制御

動脈圧受容器反射は短期血圧調節にきわめて重要な役割を果たしているが[14,15]，多くの麻酔薬が

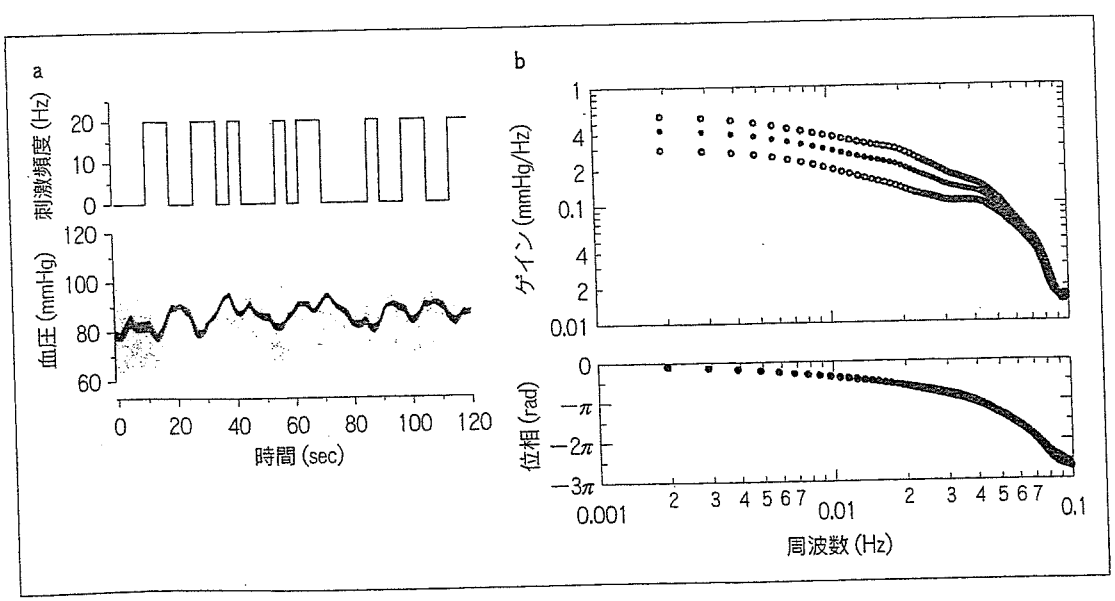

図4　脊髄交感神経の不規則刺激の例と伝達関数
a：不規則な電気刺激に対する血圧の応答は緩徐である．
b：電気刺激に対する血圧応答に関する伝達関数（$n=12$）．伝達関数により刺激に対する動脈圧応答が定量的に推定可能になる．数値は平均(●)±標準偏差(○)で示している．

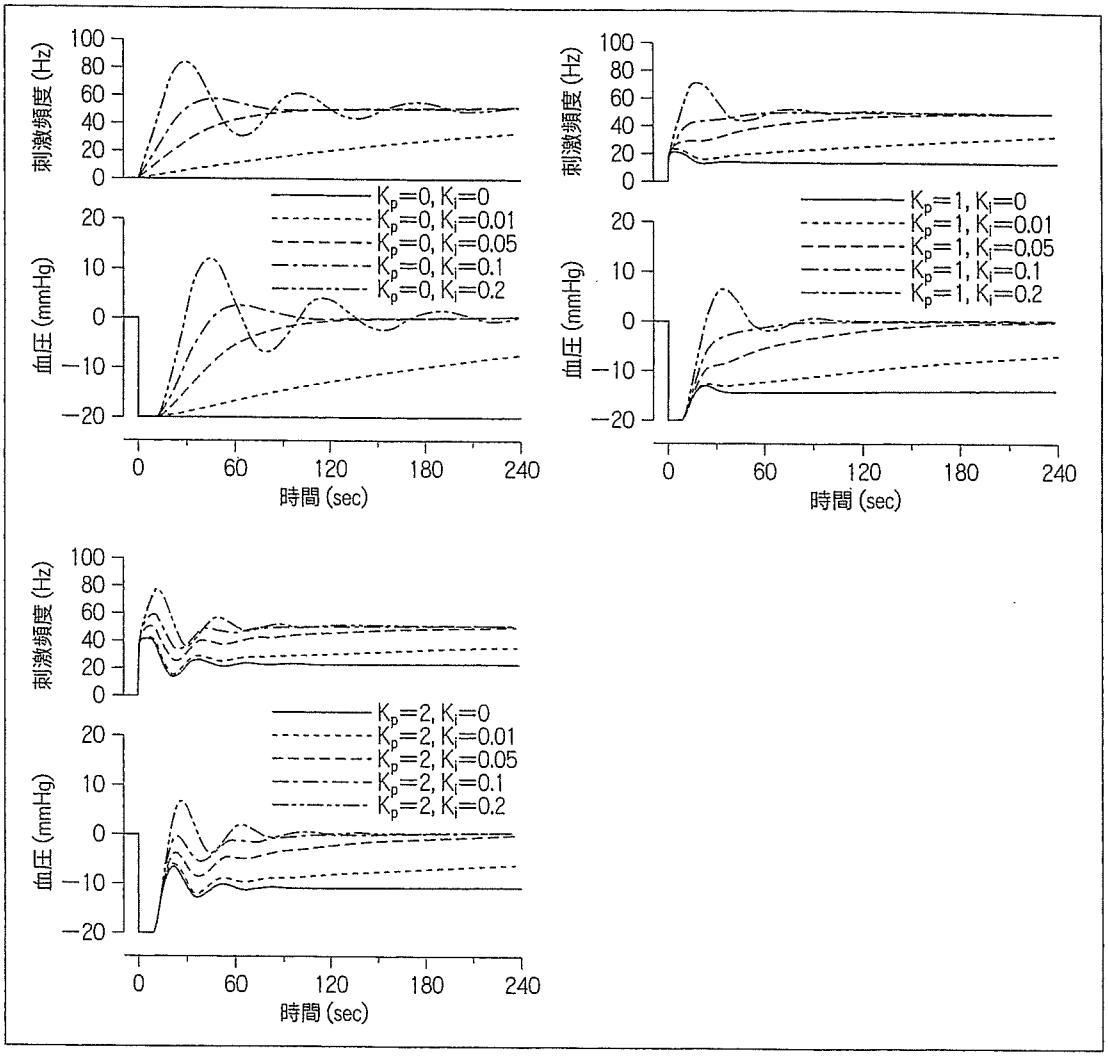

図5　数値シミュレーションによる人工的血管運動中枢の補償係数パラメータの決定
K_p と K_i はそれぞれ，比例補償係数と積分補償係数を示す．

この機能を抑制するため[16,17]，少量の出血などでも予期せぬ血圧低下をきたすことがある[18,19]．そこで，図3のように，圧センサー→コンピュータ→電気刺激装置→硬膜外カテーテル電極を用いたバイオニック圧反射装置（bionic baroreflex system: BBS）を用いて，血圧の自動制御を試みた．

1.　動作原理の開発戦略

サーボコントロールの原理を応用してBBSを試作した．サーボコントローラの動作原理としては，いわゆる，比例・積分補償型のネガティブフィードバックを採用した[20]．被制御変数である瞬時血圧 $AP(f)$ の標的血圧 $AP_t(f)$ からの偏差，すなわち，制御誤差 $E(f)$ は，$E(f)=AP_t(f)-AP(f)$ と表される．$E(f)$ から脊髄交感神経刺激 $STM(f)$ までの伝達関数 $H_1(f)$ は，比例補償係数 K_p と積分補償係数 K_i および Laplace 演算子 $s=2\pi fj$ を用いると次のように表される．

$$H_1(f)=K_p\frac{K_i}{s}$$

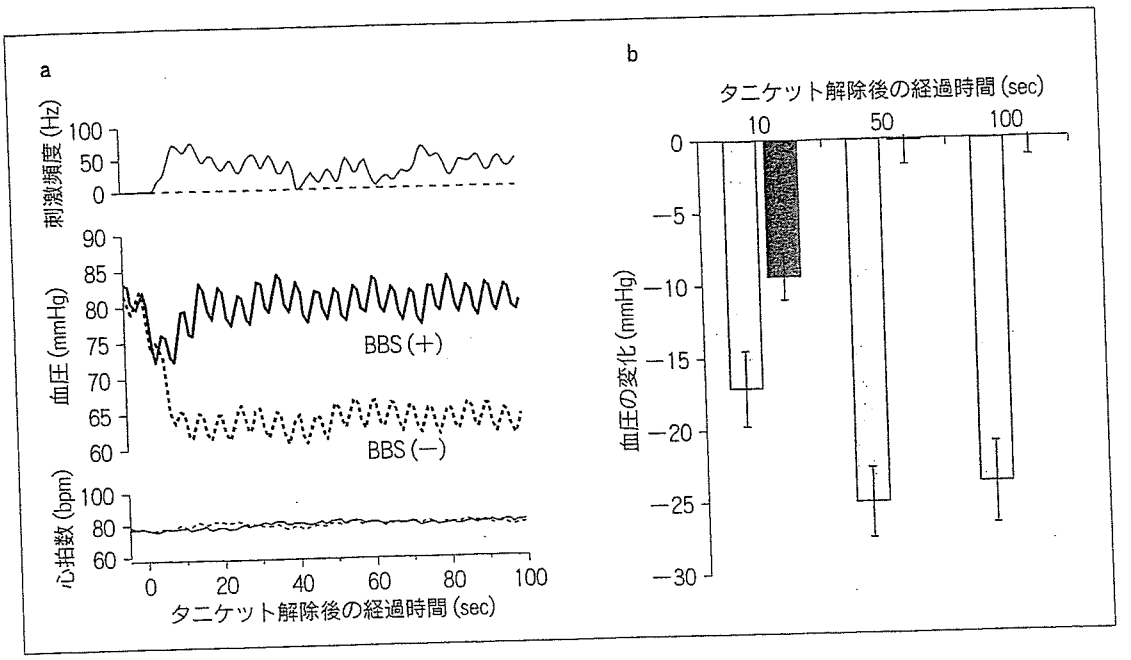

図6　バイオニック圧反射装置を用いた術中血圧制御

a：典型例.
b：21例における BBS の有効性に関する評価．BBS 未使用の場合（□）と BBS 使用の場合（▩）．数値は平均±標準偏差である.

また，脊髄交感神経刺激に対する血圧の応答特性を示す伝達関数を $H_2(f)$ とすると，被制御変数は次のように表される.

$$AP(f)=\frac{H_1(f)H_2(f)}{1+H_1(f)H_2(f)}AP_t(f)+\frac{1}{1+H_1(f)H_2(f)}AP_d(f)$$

ここで，$AP_d(f)$ は，サーボコントロールシステムに加わる外乱である．上の式から明らかなように，外乱の影響は，$1/(1+H_1(f)H_2(f))$ に抑制されることがわかる.

したがって，外乱に抗して血圧の安定化を図るためには，$H_1(f)$ の最適設計が必要である．そこで，まず，計測可能な $H_2(f)$ を次項のような方法で求め，ついで，数値シミュレーションにより $H_1(f)$ の係数 K_p および K_i を最適になるように設計した.

2.　サーボコントローラの設計

頸椎手術症例で，術中に脊髄誘発電位検査を施行予定の患者を対象にした．吸入麻酔薬による全身麻酔の導入後，経皮的に硬膜外カテーテル電極を挿入し，第9ないし第12胸椎レベルに電極を留置した．ついで刺激パルスのパラメータをパルス幅0.1ミリ秒，刺激頻度20 Hz に設定した．刺激強度は，この刺激パルスにより平均動脈圧がおおむね10 mmHg だけ上昇する電流値に調整した．筋弛緩薬投与下で，電気刺激装置に白色雑音様の不規則なトリガー信号を入力しながら，動脈圧の変動を15分間記録した．刺激パルスの頻度は，0 か 20 Hz かのいずれかになるように 8 秒間隔ごとに不規則に切り替えた．不規則刺激中の血圧応答の例を図4aに，また推定された伝達関数 $H_2(f)$ を図4bに示す．ついで，12例で求めた平均的 $H_2(f)$ を用いて，ステップ状の血圧低下（−20 mmHg）に対する血圧サーボシステムの振る舞いを比例補償係数 $K_p=0, 1, 2$，積分補償係数 $K_i=0, 0.01,$

0.05, 0.1, 0.2の組み合せでシミュレーションした．その結果，$K_p=1$, $K_i=0.1$の場合にもっとも迅速かつ安定的に血圧低下が防止されることが明らかとなった（図5）．そこで，$K_p=1$, $K_i=0.1$として人工的血管運動中枢をプログラムした．

3. BBSの有効性の検証

膝の人工関節置換術時に大腿に巻かれたタニケット（圧迫止血帯）の解除に伴う血圧低下を外乱とみなし，BBSの有効性を検証した．その結果，図6に示すように，BBSを用いることにより迅速で安全な自動血圧管理が可能であることが明らかになった[3]．

ま と め

神経インターフェイス技法に基づいたバイオニック療法が，慢性心不全に対する画期的な治療戦略となりうることを示す基礎研究結果，およびバイオニック圧反射装置により術中血圧を自動管理しうることを示唆する臨床研究結果を得ることができた．積極的に循環調節の破綻を是正したり，機能を再建することにより循環器疾患を治療するというバイオニック戦略の今後の展開に期待したい．

文 献

1) Sato T, Kawada T, Sugimachi M et al: Bionic technology revitalizes native baroreflex function in rats with baroreflex failure. Circulation 2002; **106**: 730–734
2) Li M, Zheng C, Sato T et al: Vagal nerve stimulation markedly improves long-term survival after chronic heart failure in rats. Circulation 2004; **109**: 120–124
3) Yamasaki F, Ushida T, Yokoyama T et al: Artificial baroreflex: clinical application of a bionic baroreflex system. Circulation 2006; in press
4) Pfeffer MA: Left ventricular remodeling after acute myocardial infarction. Annu Rev Med 1995; **46**: 455–466
5) Cerati D, Schwartz PJ: Single cardiac vagal fiber activity, acute myocardial ischemia, and risk for sudden death. Circ Res 1991; **69**: 1389–1401
6) Schwartz PJ, La Rovere MT, Vanoli E: Autonomic nervous system and sudden cardiac death. Experimental basis and clinical observations for post-myocardial infarction risk stratification. Circulation 1992; **85** (Suppl I): I-77–I-91
7) La Rovere MT, Bigger JT Jr, Marcus FI et al: Baroreflex sensitivity and heart-rate variability in prediction of total cardiac mortality after myocardial infarction. Lancet 1998; **351**: 478–484
8) Lechat P, Hulot JS, Escolano S et al: Heart rate and cardiac rhythm relationships with bisoprolol benefit in chronic heart failure in CIBIS II trial. Circulation 2001; **103**: 1428–1433
9) Pfeffer MA, Pfeffer JM, Steinberg C et al: Survival after an experimental myocardial infarction: beneficial effects of long-term therapy with captopril. Circulation 1985; **72**: 406–412
10) Burkoff D, Sagawa K: Ventricular efficiency predicted by an analytic model. Am J Physiol 1986; **250**: R1021–R1027
11) Zhao G, Shen W, Xu X et al: Selective impairment of vagally mediated nitric oxide-dependent coronary vasodilation in conscious dogs after pacing-induced heart failure. Circulation 1995; **91**: 2655–2663
12) Kakinuma Y, Ando M, Kuwabara M et al: Acetylcholine from vagal stimulation protects cardiomyocytes against ischemia and hypoxia involving additive non-hypoxic induction of HIF-1α. FEBS Lett 2005; **579**: 2111–2118
13) Ando M, Katare RG, Kakinuma Y et al: Efferent vagal nerve stimulation protects heart against ischemia-induced arrhythmias by preserving connexin 43 protein. Circulation 2005; **112**: 164–170
14) Sato T, Kawada T, Inagaki M et al: New analytic framework for understanding sympathetic baroreflex control of arterial pressure. Am J Physiol 1999; **276**: H2251–H2261
15) Sato T, Kawada T, Shishido T et al: Novel therapeutic strategy against central baroreflex failure: a bionic baroreflex system. Circulation 1999; **100**: 299–304
16) Tanaka M, Nishikawa T: Arterial baroreflex function in humans anaesthetized with sevoflurane. Br J Anaesth 1999; **82**: 350–354
17) Keyl C, Schneider A, Hobbhahn J et al: Sinusoidal neck suction for evaluation of baroreflex sensitivity during desflurane and sevoflurane anesthesia. Anesth Analg 2002; **95**: 1629–1636
18) Tarkkila PJ, Kauknen S: Complications during spinal anesthesia: a prospective study. Reg Anesth 1991; **16**: 101–106

19) Kahn RL, Marino V, Urquhart B et al: Hemodynamic changes associated with tourniquet use under epidural anesthesia for total knee arthroplasty. Reg Anesth 1992; **17**: 228–232

20) Kawada K, Sunagawa G, Takaki H et al: Development of a servo-controller of heart rate using a treadmill. Jpn Circ J 1999; **63**: 945–950

REGULAR PAPER

J. Physiol. Sci. Vol. 56, No. 1; Feb. 2006; pp. 95–101
Online Feb. 25, 2006; **DOI: 10.2170/physiolsci.RP002305**

Nitric Oxide Stimulates Vascular Endothelial Growth Factor Production in Cardiomyocytes Involved in Angiogenesis

Masanori KUWABARA[1,2], Yoshihiko KAKINUMA[1], Motonori ANDO[1], Rajesh G. KATARE[1], Fumiyasu YAMASAKI[3], Yoshinori DOI[2], and Takayuki SATO[1]

[1]Department of Cardiovascular Control, Kochi Medical School, Nankoku, Japan; [2]Department of Medicine and Geriatrics, Kochi Medical School, Nankoku, Japan; and [3]Department of Clinical Laboratory, Kochi Medical School, Nankoku, Japan

Abstract: Background: Hypoxia-inducible factor (HIF)-1α regulates the transcription of lines of genes, including vascular endothelial growth factor (VEGF), a major gene responsible for angiogenesis. Several recent studies have demonstrated that a nonhypoxic pathway via nitric oxide (NO) is involved in the activation of HIF-1α. However, there is no direct evidence demonstrating the release of angiogenic factors by cardiomyocytes through the nonhypoxic induction pathway of HIF-1α in the heart. Therefore we assessed the effects of an NO donor, S-Nitroso-N-acetylpenicillamine (SNAP) on the induction of VEGF via HIF-1α under normoxia, using primary cultured rat cardiomyocytes (PRCMs). Methods and Results: PRCMs treated with acetylcholine (ACh) or SNAP exhibited a significant production of NO. SNAP activated the induction of HIF-1α protein expression in PRCMs during normoxia. Phosphatidylinositol 3-kinase (PI3K)–dependent Akt phosphorylation was induced by SNAP and was completely blocked by wortmannin, a PI3K inhibitor, and N^G-nitro-L-arginine methyl ester (L-NAME), a NO synthase inhibitor. The SNAP treatment also increased VEGF protein expression in PRCMs. Furthermore, conditioned medium derived from SNAP-treated cardiomyocytes phosphorylated the VEGF type–2 receptor (Flk-1) of human umbilical vein endothelial cells (a fourfold increase compared to the control group, $p < 0.001$, $n = 5$) and accelerated angiogenesis. Conclusion: Our results suggest that cardiomyocytes produce VEGF through a nonhypoxic HIF-1α induction pathway activated by NO, resulting in angiogenesis.

Key words: vascular endothelial growth factor, angiogenesis, cardiomyocyte, Flk-1, nitric oxide.

The prognosis of patients with chronic heart failure remains poor because of progressive remodeling of the heart and lethal arrhythmia [1]. It has recently been reported that vagal nerve stimulation therapy markedly improved long-term survival in an animal model of chronic heart failure after myocardial infarction [2] and that acetylcholine (ACh) has a direct cardioprotective effect through the PI3K-Akt-hypoxia-inducible factor (HIF)-1α pathway [3, 4]. Nitric oxide (NO) is supposed to be one of the signaling molecules induced by ACh; however, it remains to be clarified whether NO is involved in angiogenesis through the nonhypoxic induction pathway of HIF-1α and vascular endothelial growth factor (VEGF), and is thereby related to the cardioprotective effects of ACh or vagal nerve stimulation.

VEGF is a key angiogenic factor and major target of HIF-1α, which is produced by ischemic tissue and growing tumors [5–7]. Factors including VEGF secreted by noncardiomyocytes are known to possess significant paracrine effects on cardiomyocytes; however, the importance of such cardiomyocyte-derived factors as paracrine or autocrine effectors on angiogenesis in the heart remains to be elucidated. The HIF-1α protein level is usually regulated by the oxygen concentration. During hypoxia, HIF-1α protein is stabilized by escaping from degradation through von Hippel-Lindau tumor-suppressor protein (VHL) [8, 9]. Furthermore, the PI3K-Akt signaling pathway, which is known for the antiapoptotic functions [10, 11], is demonstrated to be involved in HIF-1α induction [12]. Recently it has been revealed that besides hypoxia, certain cytokines, growth factors, and NO increase the HIF-1α protein level even under the normoxic conditions in some specific cells [13–15]. To our knowledge, however, the involvement of NO in this signaling pathway in cardiomyocytes under normoxic conditions remains to be elucidated. Moreover, it is also unclear whether NO is involved in angiogenesis in the heart, though NO is associated with many aspects of cellular biology involved in cell signaling, vasodilatory tone, and cell growth [16].

With this background, we speculated the nonhypoxic induction of HIF-1α in the cardiomyocytes through NO-mediated pathway and that NO plays another role in producing an angiogenic factor through the pathway. To prove this hypothesis, we assessed the effect of a NO do-

Received on Dec 2, 2005; accepted on Feb 5, 2006; released online on Feb 25, 2006; DOI: 10.2170/physiolsci.RP002305
Correspondence should be addressed to: Yoshihiko Kakinuma, Department of Cardiovascular Control, Kochi Medical School, Nankoku, Kochi, 783-8505 Japan. Fax: +81-88-880-2310, Tel: +81-88-880-2587, E-mail: kakinuma@med.kochi-u.ac.jp

nor, *S*-Nitroso-*N*-acetylpenicillamine (SNAP), on the nonhypoxic induction of HIF-1α and the VEGF production in cardiomyocytes, using the primary cultured rat cardiomyocytes (PRCMs).

MATERIALS AND METHODS

Reagents. Reagents including the NO donor, *S*-nitroso-*N*-acetylpenicillamine (SNAP), acetylcholine (ACh), a phosphatidylinositol 3-kinase (PI3K) inhibitor, wortmannin, a specific nitric oxide synthase inhibitor, N^G-nitro-L-arginine methyl ester (L-NAME), and a transcriptional inhibitor, actinomycin D, were purchased from Sigma (Sigma Chemical Co., St. Louis, Missouri, USA).

Cell culture. This study followed the guidelines of the Council for Animal Care and was approved by an ethical committee of the Laboratory Animal Center, Kochi Medical School, Nankoku, Japan. According to the guideline, the Wistar rats used in this study were sacrificed. Primary cultured rat cardiomyocytes (PRCMs) were isolated from the hearts of 2-day-old neonatal rats and incubated on a gelatin-coated dish in DMEM/Ham F12 medium including 10% horse serum and ITS supplement according to our previous studies [17]. H9c2 cells have been frequently used to study the signal transductions and channels [18, 19]. H9c2 cells have been established as cell lines derived from the rat ventricular myocytes and thus far are widely used for many biological, biochemical, and electrophysiological studies because they have characteristics similar to PRCMs. Therefore they have often been utilized instead of PRCMs in studies where tons of rat cardiomyocytes are indispensable to perform experiments. To prepare many neonatal PRCMs for RNA isolation followed by RT-PCR, we used H9c2 cells, which, along with HEK 293, derived from human embryonic kidney cells, were incubated in DMEM supplemented with 10% FBS with antibiotics. To examine the effect of SNAP, cardiomyocytes in the serum-deficient medium were treated with either 1 μM (PRCMs, HEK 293 cells) or 1 mM (H9c2 cells) of SNAP.

Determination of NO from cardiomyocytes. To determine whether ACh and SNAP release NO in cardiomyocytes, we used an NO-sensitive fluorescent dye, diaminofluorescein-2 (DAF-2) (Daiichi Pure Chemicals Co. Ltd., Tokyo, Japan) [20]. PRCMs were treated with 10 μM DAF-2 and 100 μM L-arginine for 60 min, followed by 1 μM SNAP or 1 mM ACh. To examine the effect of L-NAME on NO production, the PRCMs were first pretreated with 1 mM L-NAME for 60 min, followed by the addition of DAF-2 and L-arginine. After incubation at 37°C, the cells were washed with PBS and observed under a fluorescence microscopy.

Western blotting analysis. To investigate the signal transduction pathway from SNAP to VEGF, we evaluated the effect of wortmannin (30 nM), actinomycin D (0.5 μg/ml), and L-NAME (1 mM) on Akt, HIF-1α, and VEGF by immunoblotting assay [21, 22]. Cardiomyocytes were pretreated with one of these agents prior to the addition of SNAP. After the incubation with SNAP, the cells were lysed and the total proteins isolated. The samples were then fractionated by 10% SDS-PAGE and transferred onto a PVDF membrane. Immunoblotting was performed with the primary antibodies against HIF-1α, VEGF (Santa Cruz Biotechnology, Santa Cruz, California, USA), Akt, phospho-Akt (Cell Signaling Technology, Beverly, Massachusetts, USA), or tubulin-α (Lab Vision, Fremont, California, USA), and was then reacted with an appropriate HRP-conjugated secondary antibody. The signal was detected with an enhanced chemiluminescence system (ECL Plus, Amersham, Piscataway, New Jersey, USA). Each experiment was performed in a duplicated fashion and repeated five times (n = 5), and representative data were shown.

Transfection. To investigate the direct contribution of HIF-1α to VEGF expression, HEK 293 cells were transfected with an expression vector for dominant-negative HIF-1α (dn HIF-1α) [23], using Effectene (Qiagen, Valencia, CA, USA) according to the manufacturer's protocol. HEK293 cells are derived from human embryonic kidney cells. It is known that the transient transfection of PRCMs with a conventional method is difficult and that the efficacy is extremely low. Compared with PRCMs, HEK293 cells have been extensively used for the transient transfection of an interested gene because of the extremely high efficiency of transfection and the higher protein expression level. Therefore we used HEK293 cells. Thirty-six hours after transfection, the HEK 293 cells were pretreated with 1 μM SNAP for 12 h, followed by an evaluation of the VEGF protein level. As a control, the cells were transfected with a vector for green fluorescent protein (GFP).

Reverse transcription-PCR (RT-PCR). RNA isolation and RT-PCR were performed as described earlier [17]. The synthesized cDNA was amplified with gene-specific primers for HIF-1α, VEGF, and Glut-1, as well as β-actin. The sense and antisense gene-specific primers were as follows:

HIF-1α (sense), 5'-GGGAGAAAAGCAAGTCGTG-3',
HIF-1α (antisense), 5'-AGTCAGCAACGTGGAAGG-3';
VEGF (sense), 5'-CCAGCACATAGGAGAGATGAGCTTC-3',
VEGF (antisense), 5'-GGTGTGGTGGTGACATGGTTAATC-3';
Glut-1 (sense), 5'-ACACCTCCCCCACATACATG-3',
Glut-1 (antisense), 5'-TGGAGTTTGGCTATAACACC-3';
β-actin (sense), 5'-GAAGATCCTGACCGAGCGTG-3',
β-actin (antisense), 5'-CGTACTCCTGCTTGCTGATCC-3'.

The optimal annealing temperature and the number of cycles for each template is as follows: 54°C, 30 cycles for HIF-1α; 62°C, 34 cycles for VEGF; 62°C, 36 cycles for Glut-1; and 60°C, 32 cycles for β-actin. PCR was performed in the range that gave a linear correlation between the amount of cDNA and the yield of PCR products. The

ratio of the RT-PCR product for each gene to that of β-actin was quantified and compared.

Immunohistochemistry. After SNAP treatment, H9c2 cells were fixed with 4% paraformaldehyde for 10 min and treated with 1% Triton X-100 for another 10 min. To block nonspecific antibody binding, the cells were incubated with 5% skim milk and successively incubated with a VEGF antibody (Santa Cruz Biotechnology, Santa Cruz, California, USA) in 1% skim milk at 4°C overnight and an FITC-labeled secondary antibody (Jackson ImmunoResearch Laboratories, West Grove, PA, USA) at 4°C overnight, then examined with an immunofluorescence microscope.

Human umbilical vein endothelial cells (HUVECs) culture. To understand if NO induces the cardiomyocytes to produce a factor responsible for angiogenesis, we examined the effect of conditioned medium derived from H9c2 cells treated with SNAP on HUVECs. The HUVECs were cultured in EGM-2 culture medium supplemented with angiogenic and growth factors (Cambrex Bio Science Walkersville, Inc., Walkersville, Maryland, USA). The H9c2 cells were treated with SNAP for 2 h and then incubated in the serum-free fresh medium. After 10 hours, the supernatant was collected and added to the HUVECs by replacing EGM-2 medium. The samples were collected before and after 60 min of stimulation with conditioned medium to evaluate the phosphorylation of VEGF receptor (Flk-1), using anti–pFlk-1 antibody (Santa Cruz Biotechnology, Santa Cruz, California, USA).

To further investigate the angiogenic effect of the conditioned medium derived from cardiomyocytes, the HUVECs were cultured on Matrigel (Becton Dickinson Labware, Bedford, Maryland, USA). The 96-well plates were coated with the diluted Matrigel (50 μl/well), incubated at 37°C for 1 h, then washed with serum-free DMEM. The HUVECs (1×10^4 cells) were seeded onto each well and cultured at 37°C for 10 h in DMEM, supplemented with 20% FBS, 25 μg/ml endothelial cell growth supplement (ECGS), 10 U/ml heparin, and conditioned medium derived from SNAP-treated or nontreated H9c2 cells.

Statistical analysis. Data are presented as mean ± SE. The differences were assessed by ANOVA followed by Fisher's PLSD for multiple comparisons. The results were considered statistically significant at $p < 0.05$.

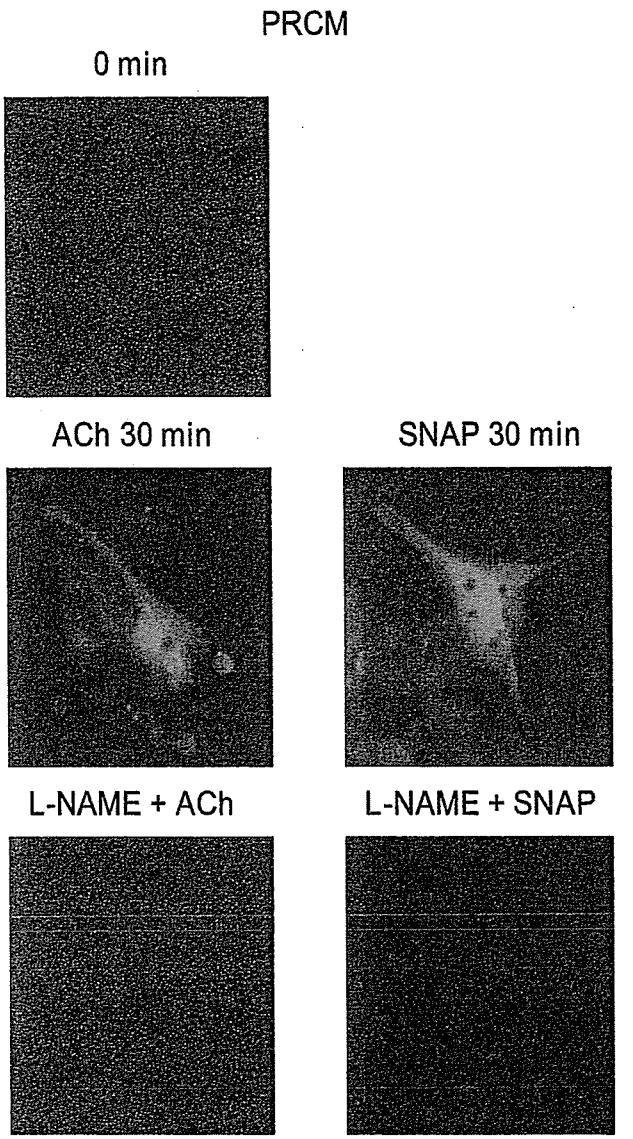

Fig. 1. Rat primary cardiomyocytes release NO in response to ACh or SNAP. PRCMs released NO after treatment with 1 mM ACh or 1 μM SNAP, evaluated with DAF-2. NO release was observed within 30 min after ACh or SNAP treatment ($n = 3$). Pretreatment with 1 mM L-NAME for 60 min blocked NO production ($n = 3$).

RESULTS

A nonhypoxic induction of HIF-1α by NO through PI3K-Akt pathway

ACh or SNAP treatment rapidly increased the NO release in PRCMs within 30 min (Fig. 1); the release was continued and peaked at 8 h. In contrast, the cells pretreated with a nitric oxide synthase inhibitor L-NAME (1 mM) failed to show the NO signal (Fig. 1). The HIF-1α protein expression was gradually increased within 8 h since the SNAP treatment (a fivefold increase compared to the baseline (0 h), $p < 0.001$, $n = 5$) in PRCMs under normoxic conditions, thus confirming the occurrence of a nonhypoxic pathway for the HIF-1α induction in the cardiomyocytes (Fig. 2a). Such an induction of HIF-1α was also observed in H9c2 cells (data not shown). To understand if this induction is regulated at the transcriptional level, we pretreated cardiomyocytes with a commonly used transcriptional inhibitor, actinomycin D (0.5 μg/ml), followed by stimulation with SNAP for 8 h. However, actinomycin D failed to inhibit the HIF-1α induction by SNAP (Fig.

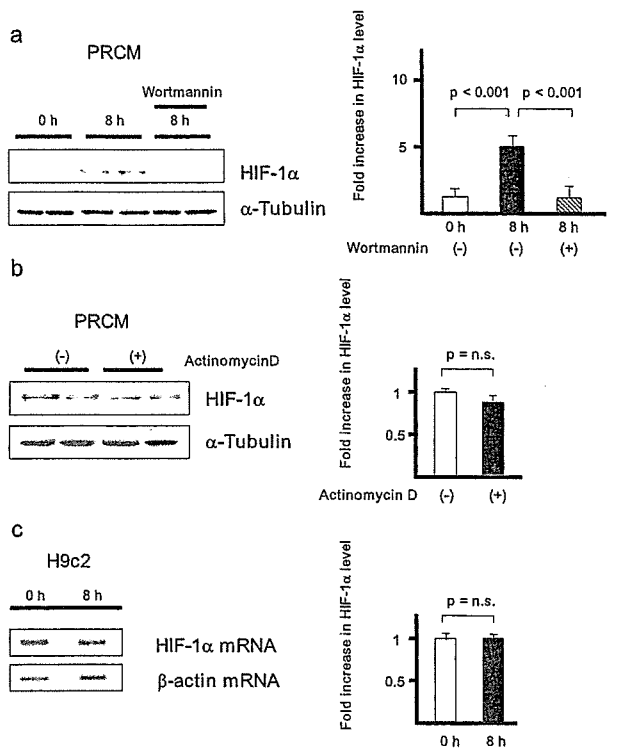

Fig. 2. The HIF-1α protein expression level is increased by SNAP in cardiomyocytes in normoxia. Treating the PRCMs for 8 h with SNAP (1 μM) already increased HIF-1α protein expression in normoxia. Pretreatment of PRCMs with wortmannin (30 nM) for 30 min inhibited SNAP-induced HIF-1α expression (n = 5) (**a**). However, treatment with actinomycin D (0.5 μg/ml) for 15 min did not inhibit the upregulation of HIF-1α protein expression by SNAP (n = 5) (**b**). In H9c2 cells, the HIF-1α mRNA expression level was not increased by SNAP (n = 5) (**c**).

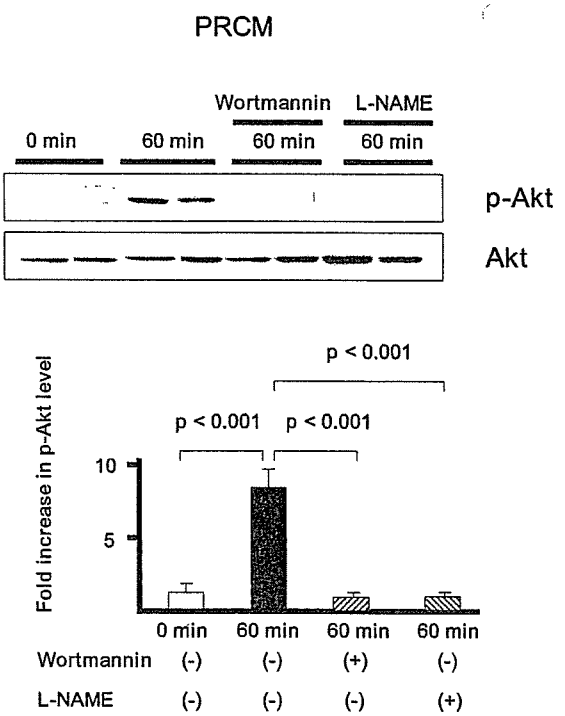

Fig. 3. Akt phosphorylation is increased by SNAP in cardiomyocytes under normoxia. Akt phosphorylation was increased by SNAP (1 μM) in PRCMs with a rapid time course. However, pretreatment with wortmannin (30 nM) for 60 min or L-NAME (1 mM) for 60 min completely inhibited the Akt phosphorylation in cardiomyocytes (n = 5).

2b), and SNAP further did not increase the HIF-1α mRNA level, evaluated by RT-PCR (Fig. 2c), thus suggesting that SNAP induces HIF-1α posttranslationally in normoxic conditions. Western blotting analysis further revealed an increased Akt phosphorylation with SNAP treatment for 60 min compared to the baseline (0 min) (an eightfold increase from the baseline, $p < 0.001$, $n = 5$) in PRCMs (Fig. 3). Pretreating the cells with PI3K inhibitor wortmannin (30 nM) or nitric oxide synthase inhibitor L-NAME (1 mM) prevented the SNAP-induced Akt phosphorylation (Fig. 3), thus demonstrating an important role for PI3K and NO in the Akt signaling pathway. Even though wortmannin (30 nM) was able to inhibit the SNAP-induced Akt or HIF-1α induction, it failed to block the NO release by the SNAP-treated cardiomyocytes (data not shown), thus confirming that NO remains upstream to the PI3K-Akt pathway. Moreover, these results also suggest the NO-dependent induction of HIF-1α in the cardiomyocytes under normoxic conditions.

Promotion of angiogenic signaling cascade by NO in cardiomyocytes under normoxia

To identify if SNAP-induced HIF-1α actually affects transcriptional activation of the target genes, the gene expression levels of the Glut-1 and VEGF were evaluated by the use of RT-PCR. The treatment of H9c2 cells with SNAP for 12 h under normoxic conditions increased the gene expressions of Glut-1 and VEGF, major HIF-1α–regulated genes (Fig. 4a). The protein expression level of VEGF was also increased following SNAP treatment, as demonstrated by the immunohistochemical and Western blotting analysis (Fig. 4 b and c). Consistent with the earlier findings, wortmannin was also able to inhibit the SNAP-induced VEGF expression in H9c2 cells and PRCMs (Fig. 4c), thus suggesting the PI3K-Akt mediated HIF-1α induction pathway in the production of VEGF by the cardiomyocytes under normoxic conditions. Furthermore, to elucidate the contribution of HIF-1α to VEGF protein expression, dn HIF-1α was introduced into HEK293 cells, and it was demonstrated that dn HIF-1α partially inhibits the VEGF induction by SNAP (Fig. 4d).

VEGF production in cardiomyocytes was further confirmed by an addition of conditioned medium derived from SNAP-treated or nontreated H9c2 cells to the HUVECs. As expected, the conditioned medium-treated cells